Deliverable

D4.2: Exposure and vulnerability models for RLA service for Europe (Report)

Deliverable information	
Work package	WP4. Effects: Advancing loss and resilience assessment for earthquake early warning and operational earthquake loss forecasting
Lead	EUCENTRE
Authors	Helen Crowley, EUCENTRE Jamal Dabbeek, EUCENTRE Sevgi Ozcebe, EUCENTRE
Reviewers	Iunio Iervolino, UNINA
Approval	Management Board
Status	Draft
Dissemination level	Public
Delivery deadline	31.08.2022
Submission date	28.08.2022
Intranet path	DOCUMENTS/DELIVERABLES/Deliverable_D4.2.pdf

This project has received funding from the European Union's Horizon 2020 research and innovation programme under grant agreement No 821115

Table of contents

Summary

An accompanying deliverable, D4.1, provides access to a set of pan-European exposure and vulnerability models for the calculation of Rapid Earthquake Loss Assessment (RELA). This deliverable, instead, describes the development and testing of these models in more detail, and plans to improve them for the demonstration activities in WP6.

1. Exposure Models (Crowley et al., 2021a)

1.1 Introduction

As part of the European Seismic Risk Model (ESRM20: Crowley et al., 2021b), exposure models comprising residential, industrial and commercial buildings (and their occupants) for 44 countries have been developed using a top-down approach based mainly on public census data. ESRM20 began as an effort within the Horizon 2020 SERA project (www.sera-eu-org) and the development of the exposure and vulnerability models has continued in the RISE project. The data and methodology used to develop these models has been described in detail in Crowley et al. (2021b) and is thus not repeated in full herein, but instead the most important aspects are summarised, together with the developments that have been undertaken to ensure these models can be used for Rapid Earthquake Loss Assessment (RELA), which requires a higher resolution of exposure.

1.2 Residential buildings

There are three main approaches that have been adopted to develop the residential exposure models:

- For most countries, public census data has been collected at the highest administrative level available. This includes Albania, Austria, Belgium, Bosnia and Herzegovina, Bulgaria, Croatia, Cyprus, France, Germany, Greece, Hungary, Iceland, Kosovo, Malta, Moldova, Montenegro, Netherlands, North Macedonia, Norway, Serbia, Slovakia, Slovenia, Spain, Switzerland, Turkey.
- In Italy, Portugal and Romania, local researchers have provided a post-processed version of the census data which has been used to develop the final exposure models.
- For other countries, including the very small ones, existing GED4GEM data (Gamba et al., 2014) on the spatial distribution of building classes has been used. This covers Andorra, Czechia, Denmark, Estonia, Finland, Gibraltar, Ireland, Isle of Man, Latvia, Liechtenstein, Lithuania, Luxembourg, Monaco, Poland, Sweden and United Kingdom.

For each country, the aggregate number of dwellings or buildings within administrative units has been obtained from the aforementioned sources and coordinates have been assigned to these admin units following the recommendations of Dabbeek et al. (2021). The attributes in the census (e.g. material, age, number of storeys) have been mapped to building classes (based on literature reviews and expert judgment) that follow the GEM Building Taxonomy (Silva et al., 2022). The evolution of seismic design codes in Europe described in Crowley et al., (2021c) has been used to assign design code levels and lateral force coefficients (see Section 2.2) to the reinforced concrete buildings as a function of their age and location. Assumptions on the areas per dwelling and the reconstruction cost per square metre have been made to assign replacement costs. Occupants have been assigned as a function of the number of dwellings, and the population distribution model from PAGER (Jaiswal and Wald, 2010) has been applied to obtain the average number of occupants in residential buildings during the day, night and transit times. During the development of the exposure models, the total number of buildings, total number of dwellings and total surface area were checked against national calibration data collected for each country.

1.3 Commercial buildings

The commercial building stock represents offices, wholesale and retail (trade), and hotels. The data available to develop commercial exposure models varies significantly across Europe, but the main two approaches that have been used can be summarized as follows:

- Data on the number of commercial buildings per sector has been directly obtained from the census or from Eurostat.
- Data on the number of businesses or enterprises per sector has been obtained from the census or from Eurostat and divided by a factor to obtain an estimate of the number of buildings.

In some cases, these data were already distributed across various administrative regions in the country. When there was no spatial distribution of the data, the labour force distribution from the census was used to spatially distribute the number of buildings and obtain the aggregate number of commercial buildings within administrative units. The coordinates assigned to these admin units follows the recommendations of Dabbeek et al. (2021). These buildings have been distributed between building classes that have been defined for each country based on literature review and expert judgment. Assumptions on the areas per commercial building and the reconstruction cost per square metre have been made to assign replacement costs. A simplifying assumption has been taken that the same number of people live and work within the same administrative unit, and thus the movement of people from their place of residence to place of work is not currently modelled. It is assumed that 40% of the working population are employed in the commercial sector (based on Eurostat statistics). The population in each admin unit has been distributed as a function of the area of commercial buildings per building class, multiplied by 0.4 (given the 40% in the commercial sector) and then the PAGER population distribution model for non-residential buildings (which also accounts for the % of population that works) has been applied. During the development of the exposure models, the total floor area of offices, wholesale and retail and hotels were checked against calibration data collected for each country.

1.4 Industrial buildings

The industrial buildings in the model cover the building stock that houses the following industries: mining/quarrying, manufacturing and construction. The total number of industrial buildings in each country was obtained following one of the following three methods:

- The total number of enterprises in each country across these industries was obtained from various sources and one enterprise was assumed to represent one building.
- The total number of industrial buildings was obtained from the census or other European sources.
- The total area of industrial buildings (obtained from Sousa et al., 2017) was divided by an average area per building (obtained from neighbouring countries).

The number of industrial buildings was then distributed spatially within the country using one of the following processes:

- For a number of European countries, it has been possible to use the 30 arc-seconds grid of surface area of industrial buildings from Sousa et al. (2017). This has been obtained by combining OpenStreetMap data with CORINE land use maps (https://land.copernicus.eu/pan-european/corine-land-cover).
- Where the latter data were not available, census data were used to distribute the buildings, either using data on the distribution of businesses, or distribution of employees in the considered industrial sectors.
- For Turkey, the distribution of number of industrial buildings across admin regions was already available in the census.

The coordinates are either the centroid of the 30 arc-seconds grid or are assigned to the administrative units following Dabbeek et al. (2021). These buildings have been distributed between

industrial building classes that have been defined for each country based on literature review and expert judgment. For the countries where the total industrial surface area is available from Sousa et al. (2017), the area per industrial building is obtained by dividing this total area by the total number of industrial buildings. In other countries (e.g., Andorra, Gibraltar, Liechtenstein) this area has been based on expert judgment and checked against similar or neighbouring countries. Assumptions on the reconstruction cost per square metre have been made to assign replacement costs. The same assumptions to distribute the population described for commercial buildings have been applied, also because 40% of the working population can be assumed to be employed in the industrial sector (based on Eurostat statistics) No calibration data was used during the development of the industrial building exposure models, but comparisons and tests with other sources (e.g. GAR15) have been undertaken as a final validation of reliability of the models.

1.5 Summary Data

The current set of European exposure models lead to an estimated 145 Million buildings in Europe which house (on average, at any given time) 460 million people, and that have a total replacement value of 50 Trillion Euros, of which 2/3 is in the residential buildings. Table 1 presents the summary exposure values for each of the 44 countries in Europe.

1.6 Spatial Disaggregation of Exposure Models

For RELA, a higher resolution of the exposure models is required as compared to that needed for ESRM20, such that a more detailed representation of the impacts can be estimated and mapped. The resolution of the residential and commercial exposure models, which is directly related to the resolution of the available census/statistics data, is shown in Figure 1.

This aspect is being tackled in the RISE project in Task 2.7 through the development of the Global Dynamic Exposure (GDE) model, which aims to describe exposure on the building level by employing a fully open big-data approach including open geographic data such as OpenStreetMap, open remote-sensing data, machine learning, and other open data like cadastral data-services. The GDE provides a server infrastructure to automatically compute exposure indicators for ~375 million buildings at a global scale (a number which is growing by approx. 150,000 buildings daily as more buildings are mapped in OpenStreetMap). Some of these indicators are shown on the OpenBuildingMap (http://www.openbuildingmap.org) and its 3D version (http://obm3d.gfz-potsdam.de).

Whilst the GDE is still being developed, a solution has been proposed to provide high resolution exposure data for RELA in any location in Europe. This solution makes use of the spatial disaggregation tool that was developed as part of the Dabbeek et al. (2021) exposure study, in collaboration with the GEM Foundation (www.globalquakemodel.org). This tool is available here: https://github.com/GEMScienceTools/spatial-disaggregation. The tool is set up to use WorldPop, a global population layer at a resolution of 30 arc-seconds, but this can easily be replaced with other datasets, such as those from the Global Human Settlement Layer (https://ghsl.jrc.ec.europa.eu/datasets.php). The tool simply disaggregates the exposure models (that should be provided in the OpenQuake-engine NRML format – see Deliverable 4.1 for access to the models in this format) onto a higher resolution grid based on the density layer provided, which can represent population, urban density or any other appropriate spatial distribution. Figure 2 shows an example of the improved spatial resolution in Spain after applying the spatial disaggregation tool.

Table 1. Summary of the number, average number of occupants (over a 24-hour period) and total replacement cost of buildings (residential, commercial and industrial) in the European exposure models (from Crowley et al., 2021a)

Country	Number of buildings (thousands)	Occupants (average) (thousands)	Replacement cost (M EUR)
Albania	644	2043	30365
Andorra	18	56	8331
Austria	2316	6572	1086647
Belgium	3847	8439	1297493
Bosnia and Herzegovina	1099	2487	62981
Bulgaria	2193	5104	290548
Croatia	1670	2961	157490
Cyprus	287	625	90447
Czechia	2373	7824	616284
Denmark	1687	4274	876430
Estonia	235	971	63904
Finland	1339	4064	606109
France	15347	47581	7448179
Germany	19935	58029	10651811
Gibraltar	6	25	3484
Greece	3352	7743	608960
Hungary	2824	7270	528346
Iceland	74	262	62178
Ireland	1929	3619	508573
Isle of Man	20	60	8244
Italy	12188	43803	5262975
Kosovo	292	1348	20031
Latvia	383	1397	95219
Liechtenstein	14	27	11205
Lithuania	599	2050	160848
Luxembourg	131	464	82029
Malta	117	376	30247
Moldova	813	1968	43351
Monaco	10	29	6857
Montenegro	165	476	15490
Netherlands	5498	12875	2596802
North Macedonia	494	1523	41134
Norway	1761	3888	878738
Poland	7025	27916	1445547
Portugal	3629	6865	706579
Romania	5507	13818	337233
Serbia	2341	5164	227816
Slovakia	996	4021	287869
Slovenia	512	1497	84052
Spain	10013	32897	3738161
Sweden	2379	7576	1318713
Switzerland	1874	6083	1294150
Turkey	9160	61765	822174
United Kingdom	15475	49256	5548205

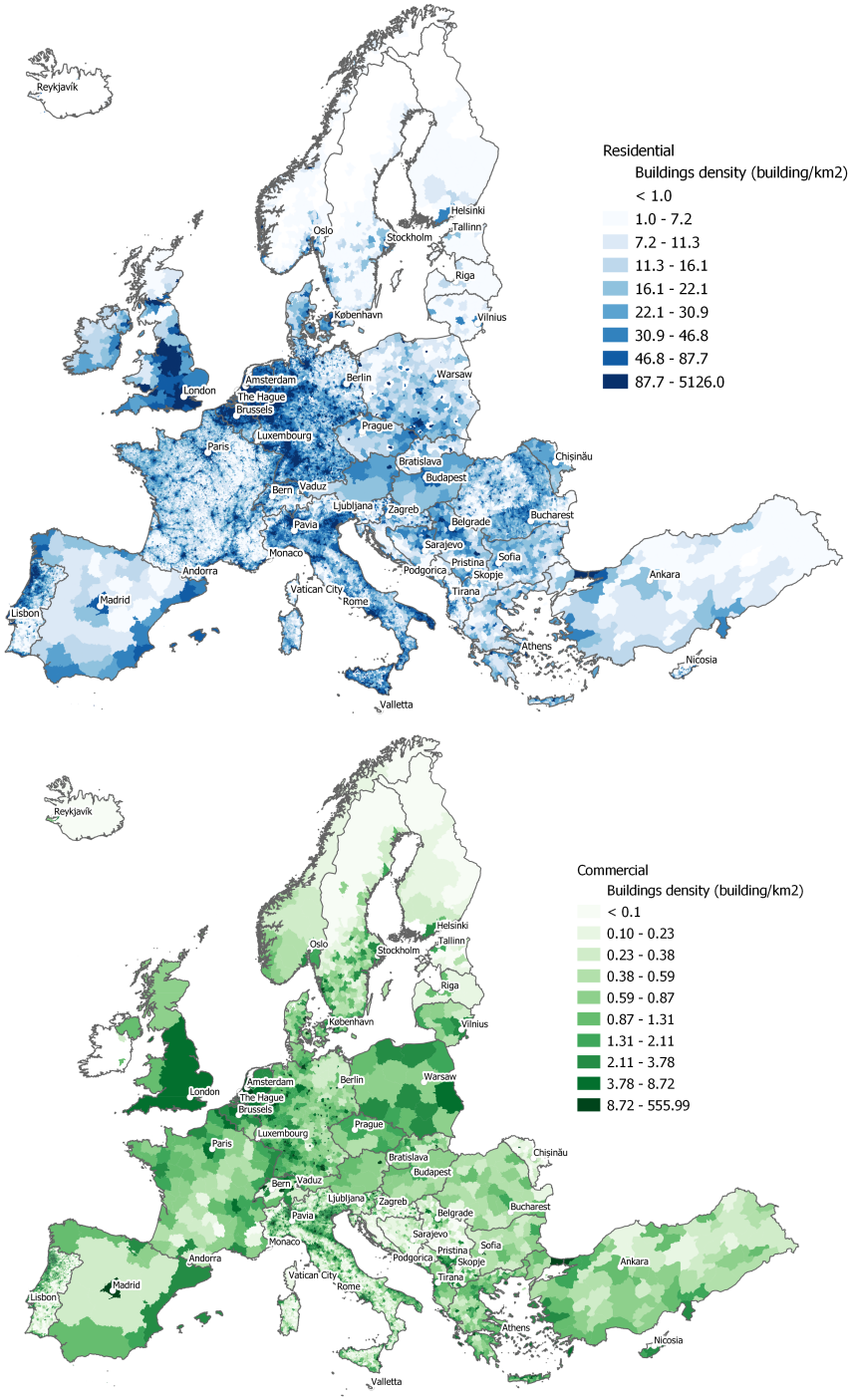

Figure 1. Highest resolution of the ESRM20 residential (top) and commercial (bottom) exposure models, shown by plotting the building density for each administrative unit.

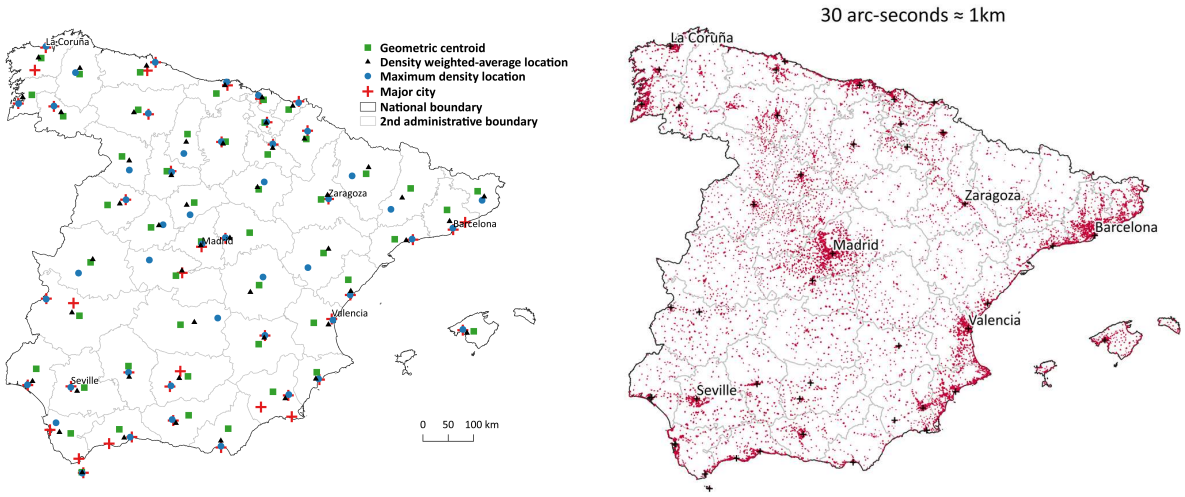

Figure 2. (Left) Original resolution of number of buildings in Spain (with varying location of assigned coordinates), (Right) 30 arc second resolution based on disaggregating the admin unit-based exposure models using Global Human Settlement layers (https://ghsl.jrc.ec.europa.eu/datasets.php) (from Dabbeek et al., 2021)

1.7 Ongoing Developments of Exposure Models

From next year, the 2021 census data is expected to become available in many European countries. This data will need to be downloaded and postprocessed for the updating of the exposure models. This will lead to the need for a more detailed assessment of the introduction of modern seismic design codes (i.e. high design code: CDH) in each European country, and the mapping of associated seismic zonation maps and the calculation of lateral force coefficients.

By releasing the models and assumptions publicly, additional feedback from the scientific community is expected. This feedback will be actively sought, in particular on the mapping schemes used in each country, to reduce any bias that might currently be included due to inaccuracies in the building classes present in each country for different occupancy classes.

Improvements to the modelling of occupants within the buildings during different times of the day, week and season, accounting also for the migration of people from their place of residence to place of work, or for tourism, is being investigated using data sets such as those from the ENACT project (Schiavina et al., 2020: https://ghsl.jrc.ec.europa.eu/enact.php). The daily and monthly population patterns from this project can be used to rescale the occupants inside the residential, commercial and industrial buildings resulting in 24 occupancy levels: day and night for 12 months. Figure 3 shows that in August more people live in the central area of Lisbon compared to its suburbs. A 5.9 Mw offshore night-time scenario has been used to calculate losses for winter (December) and summer (August) times. Figure 4 shows a reduction in the number of fatalities in the surrounding areas of Lisbon of 2% and an increase of 17% in the city centre and some coastal (mainly touristic) regions. Overall, for this scenario, the net fatalities in a summer scenario are 12% higher compared to the winter scenario.

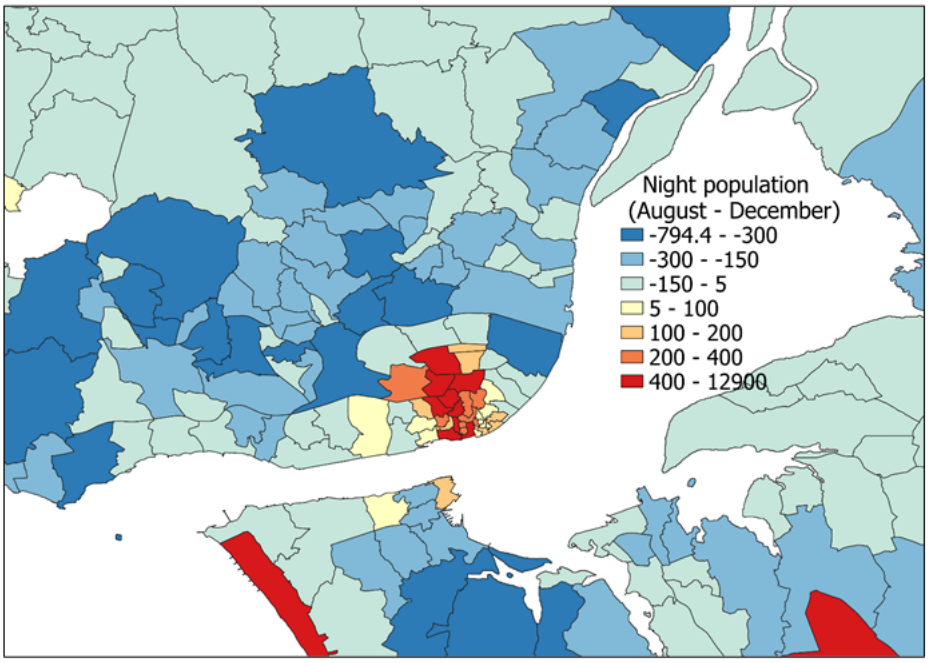

Figure 3. Difference in night-time population between August and December for Lisbon and its suburbs

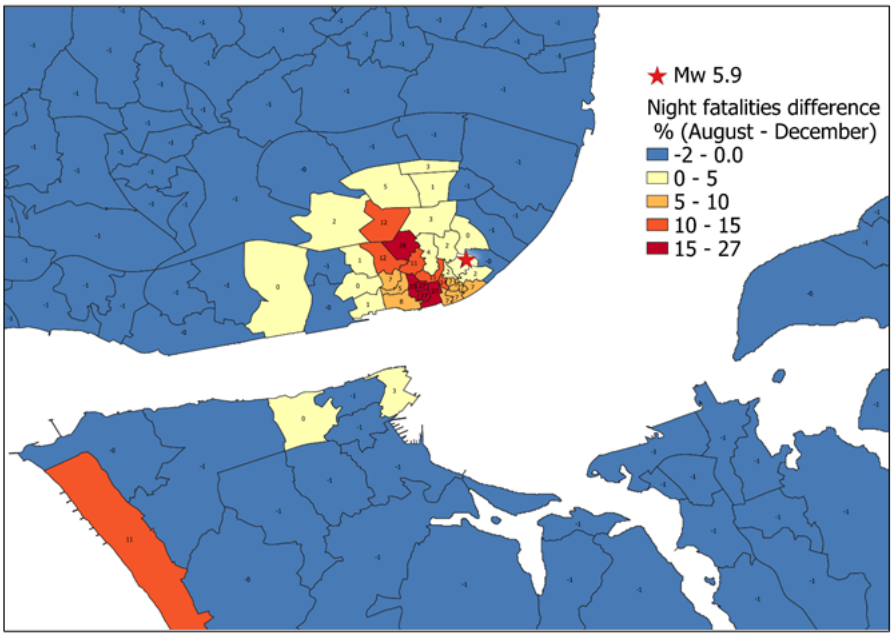

Figure 4. Percentage change in distribution of fatalities for a Mw 5.9 offshore scenario close to Lisbon

As mentioned above, the statistical (administrative unit-based) exposure models described herein have been used in the development of the high-resolution GDE model, which is being developed in Task 2.7, as will be documented in Deliverable D2.13.

Time variance aspects, such that the exposure models, can keep track of the measured or assessed damage during a sequence of events, and the change in occupants of buildings (which vary with time after the event) are needed for the demonstration activities of Work Package 6. The current proposal is to account for the latter in the following manner:

- Emergency phase displaced population = occupants of moderately, extensively and completely damaged buildings (minus fatalities)
- Initial recovery phase displaced population = occupants of extensively and completely damaged buildings (minus fatalities) [this phase initiates when people are allowed to go back into the moderately damaged buildings, after they have been assessed by an engineer].

For the demonstration activities in WP6, a full set of high resolution (i.e. spatially disaggregated) exposure models which account for the time of year (i.e. for 12 different months of the year) will be made available, together with scripts to adapt the exposure models during a sequence of events to account for the aforementioned time variance aspects.

2. Vulnerability Models (Romão et al. 2021)

2.1 Introduction

As part of the European Seismic Risk Model (ESRM20: Crowley et al., 2021b), vulnerability models for 511 building classes have been developed. Herein, the most important aspects are summarised, together with the developments that have been undertaken to allow these models to be effectively used for RELA.

2.2 Capacity Curves

Capacity curves describe the lateral strength and deformation capacity of buildings or building classes, and are often transformed to the ADRS (acceleration displacement response spectrum) format for the purposes of developing fragility functions.

Capacity curves for a large range of building classes are needed to cover the varying construction types in Europe present in the exposure models described above. The GEM Building Taxonomy v3.1 (Silva et al., 2022: https://github.com/gem/gem_taxonomy) has been used to define the vulnerability classes of European buildings with the attributes summarised below:

- Materials. CR: reinforced concrete, MR: reinforced masonry, MCF: confined masonry, MUR: unreinforced masonry, MUR-ADO: adobe, MUR-CB99: concrete block masonry, MUR-CL99: clay brick masonry, MUR-STDRE: dressed stone masonry, MUR-STRUB: rubble stone masonry, S: steel, W: wood/timber.
- Lateral load resisting systems. LDUAL: dual frame-wall system, LFINF: infilled frame, LWAL: load bearing wall, LFM: moment frame, LFBR: braced frame.
- Code Level or Ductility. CDN: absence of seismic design, CDL: low code level (designed for lateral resistance using allowable stress design), CDM: moderate code level (designed for lateral resistance with modern limit state design), CDH: high code level (designed for lateral resistance coupled with target ductility requirements and capacity design), DNO: non-ductile, DUL: low ductility, DUM: moderate ductility, DUH: high ductility.
- Height. H: number of storeys.
- Lateral Force Coefficient. The value of the lateral force coefficient, i.e. the fraction of the weight that was specified as the design lateral force in the seismic design code (see Code Level), expressed in % (currently applied to reinforced concrete moment and infilled frames only).

The GEM Foundation has released a global database of capacity curves (Martins and Silva, 2020) as part of their Global Seismic Risk Map (GEM, 2018). These curves have been derived through the compilation of data coming from research studies and experimental campaigns. In ESRM20 these capacity curves have been used to represent the European CR_LDUAL, CR_LWAL, MCF, MR, MUR, S and W typologies with different heights and ductility levels, for a total of 248 vulnerability classes.

As part of the European SERA project (www.sera-eu.org), a detailed set of capacity curves for European reinforced concrete infilled frames (CR_LFINF) and moment frames (CR_LFM) were developed (Romão et al., 2019). A total of 264 reinforced concrete classes were identified by combining different numbers of storeys (1 to 6), seismic design code levels (no code: CDN, low code: CDL, moderate code: CDM, high code: CDH) and lateral force coefficient levels (0, 5, 10, 15, 20, 25, 30 % of the weight of the structure). Buildings of design class CDN were typically designed to older

codes (from before the 1960's) that used allowable stresses and very low material strength values and considered predominantly the gravity loads. Buildings of design class CDL were designed considering the seismic action by enforcing values of the lateral force coefficient. Structural design for these codes was typically based on material-specific standards that used allowable stress design or a stress-block approach. Seismic design including modern concepts of ultimate capacity and partial safety factors (limit state design) was the basis of the CDM category of codes. The seismic action was also accounted for in the design by enforcing values for the lateral force coefficient. Finally, the CDH class refers to modern seismic design principles that account for capacity design and local ductility measures, similar to those available in Eurocode 8. As part of the study of the evolution of seismic design codes in Europe (Crowley et al., 2021c), seismic zonation maps associated with the seismic design codes employed in Europe over the last century have been used to identify the lateral force coefficient of the reinforced concrete frame building classes in the exposure models (see Chapter 1).

The capacity curves for these 264 vulnerability classes were developed through simulated design of prototype frames (e.g., Borzi et al., 2008; Verderame et al., 2010) and then nonlinear analysis has been undertaken to obtain the backbone capacity curves of these frames. Up to 300 capacity curves have been simulated per class by modifying the geometrical and material properties of the prototype frames, and thus accounting for the building-to-building variability in the simulated design, but the median capacity curves have been used to develop the fragility functions for computational efficiency (and additional dispersion has been added to the fragility and vulnerability models to account for the building-to-building variability).

2.3 Vulnerability Modeller's Toolkit

The fragility functions of the European vulnerability classes have been computed using the Vulnerability Modeller's Toolkit (VMTK), a resource that has been developed and released by the GEM Foundation in collaboration with members of the European risk community (Martins et al., 2021). This toolkit is a set of Python scripts that read the capacity curves (see Section 2.2), produce SDOF hysteretic models (based on standard hysteretic models), launch OpenSeesPy (https://openseespydoc.readthedocs.io/en/latest/) to run nonlinear dynamic analysis, apply linear censored regression to the cloud of nonlinear responses, and compute fragility functions for different damage states, based on the user-defined damage state thresholds. The complete toolkit, including source code and GUI, is currently hosted in a publicly available GitHub repository. https://github.com/GEM-ScienceTools/VMTK-Vulnerability-Modellers-ToolKit. All of the details of how GEM's Vulnerability Modeller's Toolkit (VMTK) has been applied in the development of fragility models in Europe are provided in Crowley et al. (2021b).

Damage-loss models have been applied to the fragility functions (which are provided for slight, moderate, extensive and complete damage) leading to two types of vulnerability models:

- economic loss due to direct costs to repair/replace buildings;
- loss of life of occupants due to damage/collapse of buildings.

For RELA, other risk metrics can be important for stakeholders, such as displaced people and injured people. Proposals for how to transform the fragility functions into these risk metrics are provided herein in Section 2.5.

2.4 Validation of Vulnerability Models

The economic loss and loss of life vulnerability models have been compared with national empirical models, in terms of macroseismic intensity (MMI) released by PAGER (Jaiswal et al., 2009; Jaiswal and Wald, 2013). A mean vulnerability function for a number of countries has been calculated through an exposure-weighted combination of the vulnerability models of all the building classes in

the country. For economic loss, the weighting has been based on the total replacement cost per typology, whereas for loss of life, the average occupants have been used. The vulnerability models with an intensity measure of spectral acceleration at 0.3 seconds, Sa(0.3), have been used, and the spectral ordinates have been converted to Mercalli Cancani Sieberg (MCS) intensity, using the Faenza and Michelini (2010) model (with the associated uncertainty in the conversion represented by mean and +/- 1 standard deviation vulnerability curves). It is assumed, for the purposes of these simple comparisons, that MMI and MCS are equivalent. It is noted that the vulnerability models for Sa(0.3) have been used because this is the most efficient intensity measure for many masonry building classes (and these are the predominant typology in many countries – see Crowley et al., 2021a) and also because conversions to MCS/MMI were not currently available for other spectral ordinates. Figure 5 shows this comparison in terms of economic loss vulnerability for Greece, Romania, Italy and Turkey, and Figure 6 shows this comparison in terms of fatality/loss of life vulnerability.

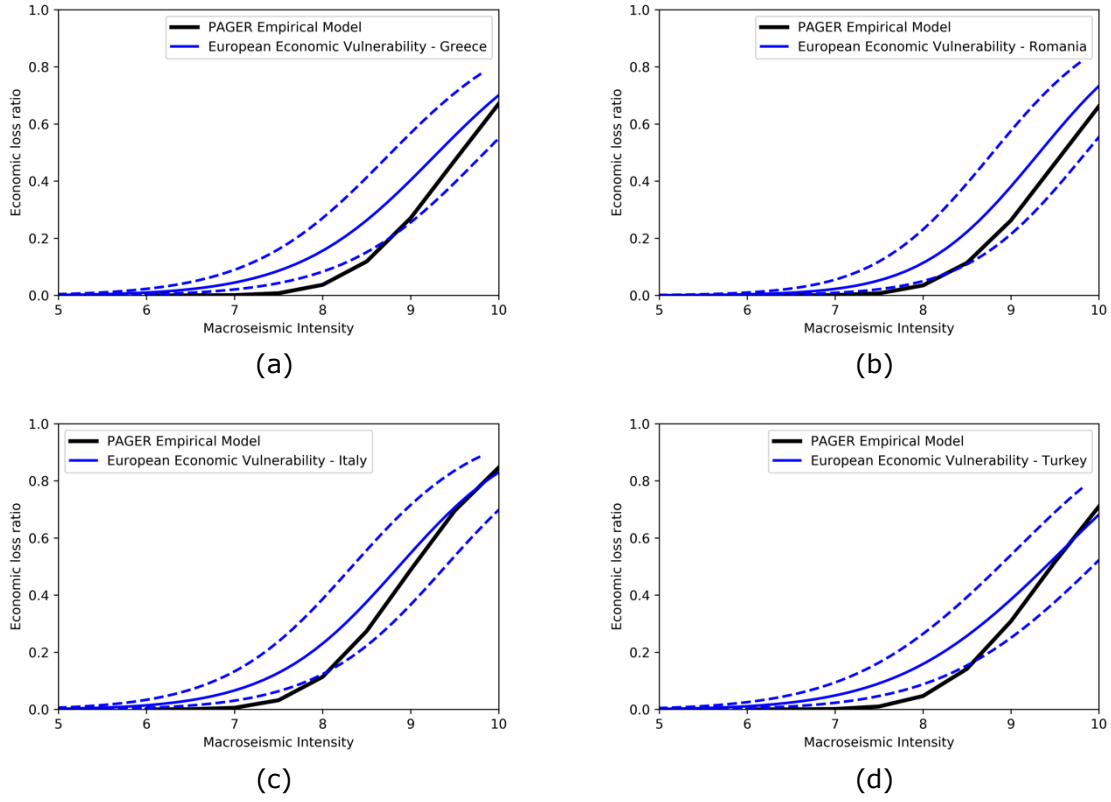

Figure 5. Comparison of national empirical vulnerability models for economic losses from PAGER with national average vulnerability models produced using the models developed herein, and converted to macroseismic intensity. The dotted lines show the mean and +/- 1 standard deviation due to the uncertainty in the conversion of spectral acceleration to macroseismic intensity.

These figures show that the analytical models developed herein for economic losses compare very well with these empirical models for all countries considered. On the other hand, there is a larger difference in the models for fatalities, which is expected given that fatalities are much rarer and the empirical data is only based on a few events per country and is highly influenced by aspects such as the time of day of the event and number of people inside the buildings at the time of the earthquake. Another issue with this comparison for fatalities is that only a few building classes in a few locations of these countries have actually caused fatalities, whereas the national models developed from the analytical models are weighted by all building classes in the country. Hence, these comparisons alone are not sufficient to test the validity of the models and further tests are required.

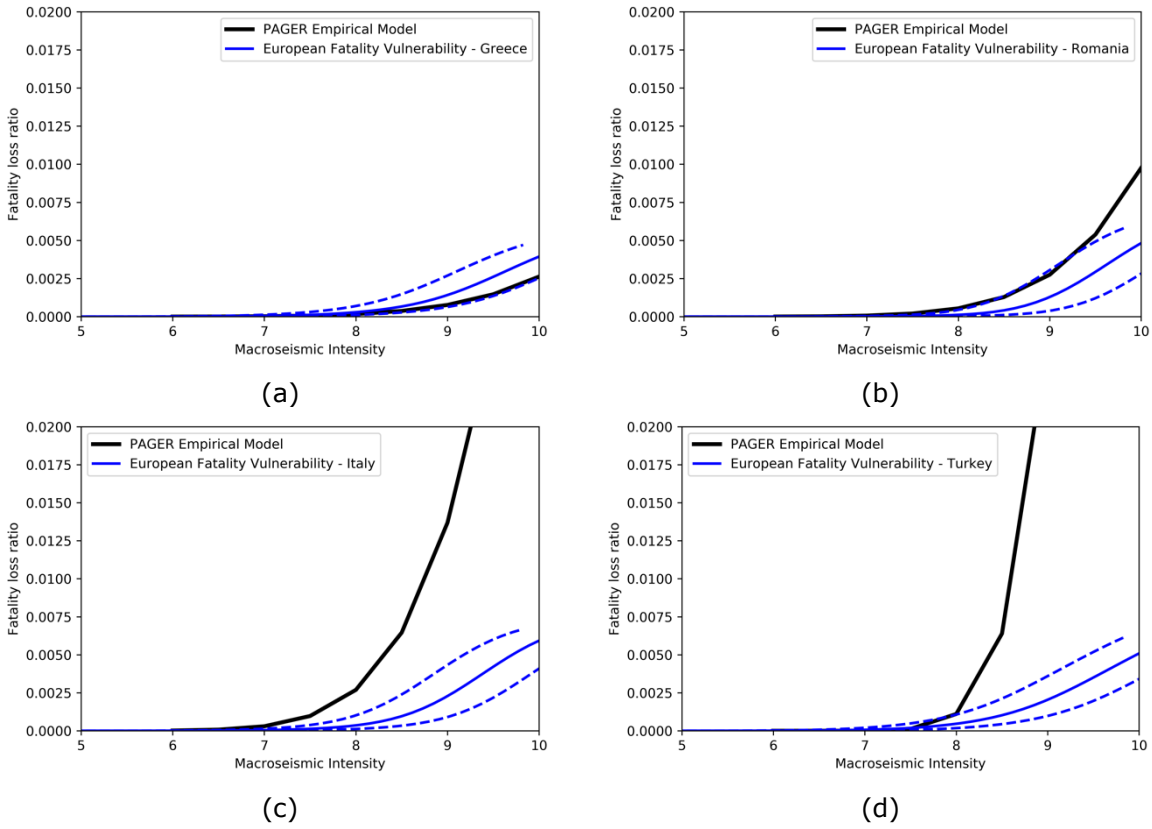

Figure 6. Comparison of national empirical vulnerability models for fatalities from PAGER with national average vulnerability models produced using the models developed herein, and converted to macroseismic intensity. The dotted lines show the mean and +/- 1 standard deviation due to the uncertainty in the conversion of spectral acceleration to macroseismic intensity.

Additional tests have therefore been undertaken to compare the losses predicted by the analytical models with past losses observed in recent damaging earthquakes in Europe. A total of 48 scenarios above magnitude 5 in Europe since the 1980's have been considered, and two approaches to represent the ground motion fields have been considered. The first uses scenario rupture models together with the European ground motion and site response models for each event (see Crowley et al., 2021a for more details). The second makes use of ShakeMaps published for these events, either by USGS (https://earthquake.usgs.gov/data/shakemap/) or, for those in Italy and neighbouring countries, from INGV (http://shakemap.rm.ingv.it/shake4/). These ground motions are then combined with the current exposure and vulnerability models in the OpenQuake-engine to estimate direct economic losses and number of fatalities. The uncertainty in the ground motions is considered in these analyses by producing at least 100 different ground-motion fields. The losses from each ground motion field can then be used to obtain the mean, median and any other fractile loss (such as the 5th and 95th percentile). These losses are then compared with the reports on economic losses and fatalities. Fatality and economic loss data can be openly obtained from various databases including the Centre for Research on the Epidemiology of Disasters (CRED)'s EMDAT database (EMDAT, n.d.) and NOAA's Significant Earthquake Database (NGDC/WGS, n.d.). In the plots shown in Figure 7 below, the data from CRED's EMDAT database (EMDAT, n.d.) has been used and is compared with the mean loss for each event (shown by a circle), together with the bounds given by the 5th and 95th percentile loss. A best-fit linear curve (shown by the black line) has also been fit to the modelled data.

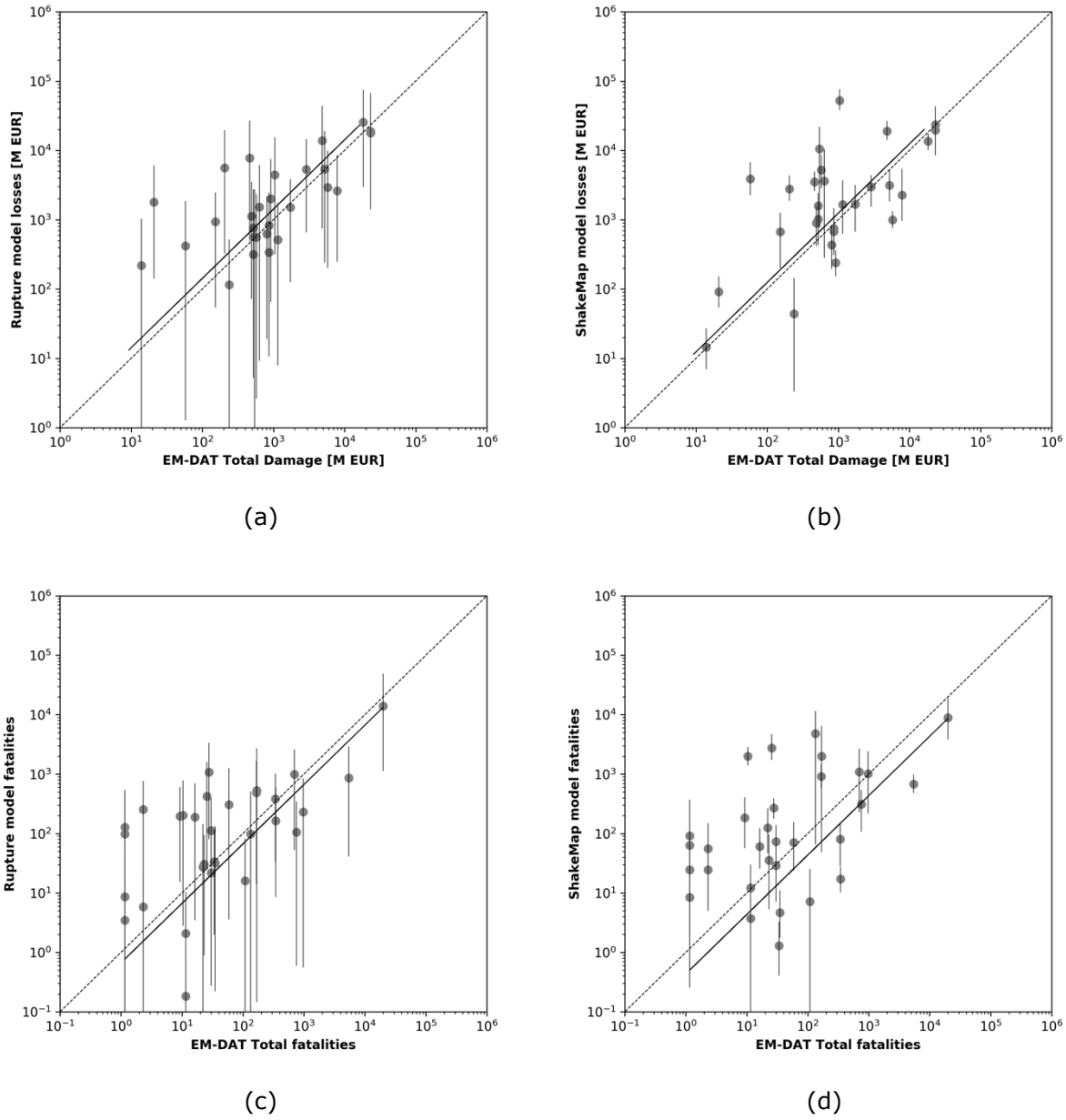

Figure 7. Comparison of observed (horizontal axis) and modelled (vertical axis) losses (a) economic losses based on rupture model, (b) economic losses based on ShakeMap model, (c) fatalities based on rupture model, (d) fatalities based on ShakeMap model

The observed economic losses in the plots have been inflated to the 2020 value using the Consumer Price Index (CPI) values reported by EM-DAT. The best-fit lines show there is a slight bias in the results, with modelled economic losses being slightly higher on average than the observed losses. For the fatalities, there appears to be a slight underestimation of the modelled losses, which could be due to changes in construction since the time of the event (and an almost 'natural selection' of the most vulnerable or fatal buildings in earthquake-hit areas).

The large uncertainties in the rupture models are evident from this plot, but the uncertainty bounds also illustrate that the combination of ground motion uncertainty, exposure and vulnerability leads, in the majority of cases, to a range of feasible losses that encompass the observed losses (i.e., those cases where the uncertainty bounds cross the 1:1 line). The uncertainties in the losses from the ShakeMaps are much lower (due to the constraints on ground motion provided by the recordings or macroseismic intensity), and thus should provide a better picture of the performance of the exposure and vulnerability models, which although are seen to produce limited bias in the losses on average, can lead to losses that are quite different from the observations in individual cases. It is worth considering that there are a lot of uncertainties in the observed losses used in these tests

(e.g. the total economic losses after an event are difficult to define and might not represent the same assets considered in the European risk model, fatalities are often misreported, and past losses have been inflated to today's value without explicitly considering the changes in the built environment).

2.5 Displaced and injured people

As mentioned above, additional metrics are needed for RELA beyond those considered in ESRM20. This includes estimates of displaced and injured people. The current proposal to account for the number of displaced people is to take the occupants of moderately, extensively and completely damaged buildings (minus fatalities). Hence, a vulnerability model in terms of the ratio of number of displaced people to number of occupants can be obtained for each building class by taking a weighted average of the fragility functions for moderate, extensive and complete damage.

For injured people, the model of Spence (2007) is proposed to be applied. Figure 8 presents the injury classification scheme and Figure 9 presents the ratios of occupants of collapsed buildings that are assumed to fall into each injury category, as a function of the building material. Assumptions on the proportion of completely damaged buildings that would collapse have already been applied to develop the loss of life vulnerability models introduced above, and so these same assumptions can be applied before assigning these ratios to produce injury vulnerability models.

Category (I)		Type of injuries		AIS
1	uninjured/ lightly injured	Head or Face	bruising/ contusions, minor cuts	2
		Abdomen	bruising, minor cuts	1
		Upper Extremities	bruising, minor cuts, sprains	1
		Lower Extremities	bruising, minor cuts, sprains	1
2	moderately injured	Head or Face	Cuts into soft tissues	2-3
		Abdomen	Cuts into soft tissues	2-3
		Upper Extremities	Dislocation, cuts into soft tissues	2-3
		Lower Extremities	Dislocation, cuts into soft tissues	2-3
		Other	Dehydration/ exposure; burns 1-2^{o}; unconscious < 1hr	3
3	seriously injured	Head or Face	Open head or facial wounds, fractures, brain concussion	3-4
		Abdomen	Pneumothorax and rib factures, crushing > 3hrs, puncture organs	1-4
		Upper Extremities	Fractures- open, displaced or comminuted (pulverised)	3
		Lower Extremities	Fractures- open, displaced or comminuted (pulverised)	3
		Other	Uncontrolled bleeding; burns 2-3^{o} (% of body?) ; unconscious > 1hr	3-5
4	critical	Head or Face	Internal head trauma, severe crushing, brain damage	5
		Abdomen	Spinal column injuries, internal organ failures due to crushing	5
		Upper Extremities	Traumatic amputations, arms	5
		Lower Extremities	Traumatic amputations, legs	5
		Other	Nerve injuries	5

Figure 6. Injury classification scheme proposed by Spence (2007) (excluding death = I_5)

	UI	I_1	I_2	I_3	I_4
Timber (1F)	45.7%	40.0%	12.0%	1.5%	0.1%
Timber (2&3F)	43.9%	40.0%	12.5%	1.5%	0.1%
Timber (>4F)	43.6%	40.0%	13.0%	2.0%	0.1%
Masonry (1F)	23.6%	50.0%	12.0%	8.0%	0.4%
Masonry (2&3F)	16.5%	50.0%	15.0%	10.0%	0.5%
Masonry (>4F)	9.4%	50.0%	18.0%	12.0%	0.6%
RC (1F)	32.9%	30.0%	19.0%	3.0%	0.2%
RC (2&3F)	20.8%	30.0%	23.0%	4.0%	0.2%
RC (>4F)	9.7%	30.0%	27.0%	5.0%	0.3%
Steel (1F)	38.9%	30.0%	15.0%	2.0%	0.1%
Steel (2&3F)	25.1%	30.0%	19.0%	3.0%	0.2%
Steel (>4F)	10.0%	30.0%	23.0%	4.0%	0.2%

Figure 7. Injury distributions for specific building types. UI = uninjured; I1 for slight injuries; I2= moderate injuries; I3 = serious injuries; I4 = critical injuries, from Spence (2007)

2.6 Next Developments to Vulnerability Models in the RISE project

For the demonstration activities in WP6, a full set of vulnerability models for displaced people and injured people (in the OpenQuake-engine format) will be made available based on the assumptions outlined herein. All of the models further developed in the RISE project will be made publicly available on the GitLab repository (see Deliverable D4.1).

3. Concluding Remarks

This deliverable has described the development and testing of pan-European exposure and vulnerability models that have been made publicly available (see Deliverable D4.1). The plans to improve these models for the demonstration activities in WP6 have been outlined. This includes improving the spatial resolution and population distribution of exposure models and more risk metrics for the vulnerability models. All resulting models will be shared on the GitLab repositories (see D4.1) before the end of the project.

References

Borzi B., Crowley H. and Pinho R. (2008) "Simplified pushover-based vulnerability analysis for large-scale assessment of RC buildings," Engineering Structures, 30, pp. 804-820.

Crowley H., Despotaki V., Rodrigues D., Silva V., Costa C., Toma-Danila D., Riga E., Karatzetzou A., Fotopoulou S., Sousa L., Ozcebe S., Gamba P., Dabbeek J., Romão X., Pereira N., Castro J.M., Daniell J., Veliu E., Bilgin H., Adam C., Deyanova M., Ademović N., Atalic J., Bessason B., Shendova V., Tiganescu A., Toma-Danila D., Zugic Z., Akkar S., Hancilar U. (2021a). European Exposure Model Data Repository (v1.0), Data set, Zenodo, http://doi.org/10.5281/zenodo.4062044.

Crowley H., Dabbeek J., Despotaki V., Rodrigues D., Martins L., Silva V., Romão X., Pereira N., Weatherill G., Danciu L. (2021b) European Seismic Risk Model (ESRM20). EFEHR Technical Report 002 V1.0.0, https://doi.org/10.7414/EUC-EFEHR-TR002-ESRM20

Crowley H., Despotaki V., Silva V., Dabbeek J., Romão X., Pereira N., Castro J.M., Daniell J., Veliu E., Bilgin H., Adam C., Deyanova M., Ademović N., Atalic J., Riga E., Karatzetzou A., Bessason B., Shendova V., Tiganescu A., Toma-Danila D., Zugic Z., Akkar S., Hancilar U. (2021c) "Model of Seismic Design Lateral Force Levels for the Existing Reinforced Concrete European Building Stock", Bulletin of Earthquake Engineering, https://doi.org/10.1007/s10518-021-01083-3.

Dabbeek J., Crowley H., Silva V., Weatherill G., Paul N., Nievas C. (2021) "Impact of exposure spatial resolution on seismic loss estimates in regional portfolios," Bulletin of Earthquake Engineering, https://doi.org/10.1007/s10518-021-01194-x

EMDAT (n.d.) International Disasters Database of the Centre for Research on the Epidemiology of Disasters, Available at: https://www.emdat.be/ (accessed 15 September 2021).

Faenza L. and Michelini A. (2010) "Regression analysis of MCS intensity and ground motion parameters in Italy and its application in ShakeMap," Geophysical Journal International, 180(3), pp. 1138–1152.

Gamba P., Cavalca D., Jaiswal K., Huyck C. and Crowley H. (2014) "The GED4GEM project: Development of a global exposure database for the global earthquake model initiative," Proceedings of the 15th World Conference on Earthquake Engineering, Lisbon, Portugal.

GEM (2018) Global earthquake maps, Available at: www.globalquakemodel.org/gem (accessed 6 December 2018).

Global Assessment Report (GAR) (2015) UNISDR 2015 Global Assessment Report, Available at: www.preventionweb.net/english/hyogo/gar/2015 (accessed 21 November 2021).

Jaiswal K., Wald D. and Hearne M. (2009) Estimating casualties for large worldwide earthquakes using an empirical approach, US Geological Survey Open-File Report 1136.

Jaiswal K. and Wald D. (2010) "Development of a semi-empirical loss model within the USGS Prompt Assessment of Global Earthquakes for Response (PAGER) System," Proceedings of the 9th US and 10th Canadian Conference on Earthquake Engineering: Reaching Beyond Borders, Toronto, Canada.

Jaiswal K. and Wald D. (2013) "Estimating Economic Losses from Earthquakes Using an Empirical Approach," Earthquake Spectra, 29(1), pp. 309-324.

Martins L. and Silva V. (2020) "Development of a fragility and vulnerability model for global seismic risk analyses," Bulletin of Earthquake Engineering, https://doi.org/10.1007/s10518- 020-00885-1

Martins L., Silva V., Crowley H. and Cavalieri F. (2021) "Vulnerability Modeller's Toolkit, an Open-Source Platform for Vulnerability Analysis," Bulletin of Earthquake Engineering, https://doi.org/10.21203/rs.3.rs-458348/v1

National Geophysical Data Center / World Data Service (NGDC/WDS): NCEI/WDS Global Significant Earthquake Database. NOAA National Centers for Environmental Information. doi:10.7289/V5TD9V7K (accessed 21 November 2021)

Romão X., Castro J.M., Pereira N., Crowley H., Silva V., Martins L. and Rodrigues D. (2019) European physical vulnerability models, SERA Deliverable D26.5, Available at: http://static.seismo.ethz.ch/SERA/JRA/SERA_D26.5_Physical_Vulnerability.pdf.

Romão X., Pereira N., Castro J.M., Crowley H., Silva V., Martins L., and De Maio F. (2021) European Building Vulnerability Data Repository (v2.1), Data set, Zenodo, https://doi.org/10.5281/zenodo.4062410.

Schiavina M., Freire S., Rosina K., Ziemba L., Marin Herrera M., Craglia M., Lavalle C., Kemper T., Batista e Silva F. (2020) ENACT-POP R2020A - ENACT 2011 Population Grid. European Commission, Joint Research Centre (JRC).

Silva V., Brzev S., Scawthorn C., Yepes-Estrada C., Dabbeek J. and Crowley H. (2022) "A Building Classification System for Multi-Hazard Risk Assessment," International Journal of Disaster Risk Science, 13, 161–177 DOI: https://doi.org/10.1007/s13753-022-00400-x

Spence R. (ed) (2007) "Earthquake Disaster Scenario Predictions and Loss Modelling for Urban Areas," LESSLOSS Report No. 2007/07

Sousa L., Silva V., Bazzurro P. (2017) "Using open-access data in the development of exposure data sets of industrial buildings for earthquake risk modeling," Earthquake Spectra, 33, pp. 63–84, https://doi.org/10.1193/020316eqs027m.

Verderame G.M., Polese M., Marinello C. and Manfredi G. (2010) "A simulated design procedure for the assessment of seismic capacity of existing reinforced concrete buildings," Advances in Engineering Software, 41(2), pp. 323- 335.